FEATURE ARTICLE

Simultaneous Time- and Wavelength-Resolved Fluorescence Microscopy of Single Molecules

A. Khai Luong,* Claudiu C. Gradinaru, David W. Chandler, and Carl C. Hayden
Sandia National Laboratories, 7011 East Avenue, MS 9055, Livermore, California 94550
Received: January 26, 2005; In Final Form: April 22, 2005

Single fluorophores and single-pair fluorescence resonance energy transfer were studied with a new confocal fluorescence microscope that allows, for the first time, the wavelength and emission time of each detected photon to be simultaneously measured with single molecule sensitivity. In this apparatus, the photons collected from the sample are imaged through a dispersive optical system onto a time and position sensitive photon detector. For each detected photon the detection system records its wavelength, its emission time relative to the excitation pulse, and its absolute emission time. A histogram over many photons can generate a full fluorescence spectrum and correlated decay plot for a single molecule for any time interval. At the single molecule level, this approach makes possible entirely new types of temporal and spectral correlation spectroscopies. This paper presents our initial results on simultaneous time- and wavelength-resolved fluorescence measurements of single rhodamine 6G (R6G), tetramethylrhodamine (TMR), and Cy3 molecules embedded in thin films of poly(methyl methacrylate) (PMMA), and of single-pair fluorescence resonance energy transfer between two Alexa fluorophores spaced apart by a short polyproline peptide.

Introduction

Single molecule fluorescence microscopy is a sensitive probe of the nanoenvironment surrounding the fluorescing molecule. Various fluorescence characteristics, such as the fluorescence intensity, spectrum, lifetime, and polarization, have been exploited to monitor interactions of molecules with their immediate surroundings.[1] These measurements on single molecules directly probe the heterogeneity of a sample and the local environments within it. Single molecule dynamics, such as molecular conformational changes, excited-state energy transfer, or quenching, can also be studied by measuring the time dependence of fluorescence characteristics such as the spectrum, lifetime, or FRET (fluorescence resonance energy transfer) efficiency.[2−4] Experiments on samples of individual molecules measure distributions of single molecule properties and rates of dynamic processes that are usually averaged in ensemble measurements.

Many sensitive, powerful techniques for measurements of fluorescence from single molecules have been developed based on various forms of time-resolved single-photon counting. Time-correlated single-photon counting (TCSPC) with fast-pulsed lasers provides measurements of fluorescence lifetimes with excellent time resolution.[5−8] Furthermore, continuous recording of the sequence of absolute photon arrival times (time stamping) has become a powerful technique for studying fluorescence fluctuations with high temporal resolution.[9−11] The complete record of photon arrival times can be used to study dynamics of the fluorescent system over a wide range of time scales. Both absolute arrival times and emission times relative to a pulsed laser can be simultaneously recorded to study, for example, fluorescence lifetime fluctuations.

By simultaneously probing multiple parameters of the sample fluorescence, one can more thoroughly characterize the single molecule system. In particular, some of the motivations for developing single molecule multiparameter measurements are the following: (1) to identify single fluorophores within a multiple-fluorophore sample based on a range of fluorescence characteristics,[12] (2) to fully characterize the fluorescence properties of the molecule to obtain the most complete information on its local environment and the dynamics of the molecule within this environment, and (3) to gain insights into mechanisms that control the fluorescence properties by measuring correlations between fluorescence spectra, decay times, and intensities. The ability to measure these correlations is valuable for understanding both the fundamental photodynamics of the excited molecule and how the fluorescence reports on the local environment. Many factors determine the fluorescence characteristics, such as the local host environment, the orientation of the fluorophore relative to the excitation laser polarization, the internal electronic states of the fluorophore, and energy transfer from the excited fluorophore to a nearby acceptor fluorophore or quencher. Determining how these factors influence fluorescence-based measurements is important for the application of single molecule spectroscopy to probing local environments. For example, single-pair fluorescence resonance energy transfer (spFRET) is a technique in which a donor fluorophore is excited and can transfer energy to a nearby acceptor fluorophore. This energy transfer is very sensitive to the separation of the donor and acceptor fluorophores, so measuring the relative fluorescence yield from these two species provides a measure of the distance between them. This method, which is widely used as a sensitive ruler at the 2−10 nm scale, can be critically affected by the fluorescence dynamics. Time-resolved multiparameter fluorescence measurements can directly and simultaneously monitor factors such as spectral shifts and lifetime changes that influence spFRET efficiency.

* Corresponding author. Telephone: (925) 294-3245. Fax: (925) 294-2276. E-mail: akluong@sandia.gov.

10.1021/jp050465h CCC: $30.25
Published on Web 07/19/2005

A. Khai Luong was born in Ho Chi Minh City, Vietnam. She obtained her B.S. in Chemistry at the University of California, Davis, in 1995 and her M.S. and Ph.D. in Chemistry at the University of California, San Diego in 1998 and 2001, respectively. Under the guidance of Dr. Robert E. Continetti, she studied photodissociation dynamics of small anions in the gas phase using a photoelectron−photofragment coincidence spectroscopy technique developed in the Continetti lab. Dr. Luong joined Sandia National Laboratories in Livermore, California in 2001 as a post-doctoral research associate with Dr. Tom Kulp, developing a remote optical sensor to map natural gas leaks. From 2002 to present, Dr. Luong has worked on the development of the novel simultaneous time- and frequency-resolved fluorescence spectroscopy for single molecule studies. Her research interest is on multiparameter single-molecule spectroscopy of biomolecules to study protein and enzyme dynamics.

Claudiu C. Gradinaru was born in Bacau, Romania. He obtained his B.S. degree in Physics from University of Bucharest, Romania. He got his Ph.D. degree in Physics at the Free University of Amsterdam, in the Netherlands. His Ph.D. work in the biophysics group of Prof. Rienk van Grondelle included time-resolved ultrafast spectroscopy experiments aimed at the understanding the relation between molecular structure and efficient energy transfer in photosynthesis. In 2001 he became a postdoc in the microscopy lab of Prof. Thomas Schmidt at Leiden University in the Netherlands, where he became involved with single-molecule research and developed multiplexed scanning-probe imaging of biomembranes and living cells. Since 2003, he is a postdoc at Sandia National Labs in Livermore, California, where he is using time-resolved microspectroscopy to study photodynamics of single fluorophores, such as their response to environmental changes and resonant energy transfer, with further application to the study of protein folding dynamics and protein−protein interactions.

Several methods for multiparameter fluorescence measurements of single molecules have been previously developed. Multiwavelength fluorescence measurements with single molecule sensitivity have been achieved using multiple avalanche photodiode detectors (APDs) and various filter schemes, providing fluorescence detection with high time resolution in two to four spectral windows.[12−14] This approach has been applied for spFRET measurements.[15−18] The number of spectral windows is limited due to the increased complexity of the experiment as the number of discrete APD detectors employed is increased.

Dave Chandler was born in Albuquerque New Mexico. He received his B.S. degree in Chemistry from the University of New Mexico in 1975 and his Ph.D. in Chemistry in 1979 from Indiana University, where he worked under Dr. George Ewing studying vibrational energy transfer in cryogenic liquids. Following graduate school he accepted a postdoctoral fellowship in the laboratory of Dr. Richard N. Zare at Stanford University, where he studied unimolecular reactions after excitation of a high vibrational overtone transition. He joined the Combustion Research Facility at Sandia National Laboratory in 1982 and was promoted to Senior Scientist in 2000. He was elected as a Fellow of the American Physical Society in 1989 and, together with Dr. Paul Houston, received the Herbert P. Broida Award from the APS in 2001 for the development of the "ion imaging" technique. Ion imaging is the use of time- and position-sensitive ion detectors to accurately measure the velocity of laser-generated ions. Dr. Chandler's research interest have centered around the utilization of multiplex detection techniques, such as ion imaging, for the study of chemical dynamics both unimolecular photodissociation and bimolecular collision dynamics. He has performed extensive measurements of differential cross sections, alignment, and orientation of products of photodissociation and inelastic collisions between molecules and atoms under single-collision conditions. Most recently he has utilized crossed molecular beam scattering to cool molecules by collisions to temperatures in the milliKelvin range. Other research interests include nonlinear spectroscopy and single-molecule spectroscopy of biologically interesting systems.

Carl Hayden received his B.A. in Chemistry from the University of Colorado at Boulder. He got his Ph.D. in Physical Chemistry from the University of California, Berkeley, working with Prof. Yuan T. Lee on experimental studies of reactive scattering. His postdoctoral work at University of Wisconson, with Prof. Fleming Crim, involved detailed studies of dissociation reactions of laser excited molecules. He joined Sandia National Laboratories in 1988 working in the Combustion Chemistry Department. Since coming to Sandia, his research interests have included unimolecular reaction dynamics in highly excited molecules, femtosecond time-resolved photoion/photoelectron coincidence spectroscopies, nonlinear optical diagnostics development, and time-resolved single-molecule spectroscopy.

Many variations of this approach have been reported, including, for example, a technique using two APDs to record the fluorescence intensity, lifetime, and anisotropy.[13,19,20] Techniques employing charge-coupled-device (CCD) cameras, which typically integrate photons over a many millisecond time interval, have also been developed for single molecule multiparameter fluorescence measurements.[21−23]

Several techniques have previously been reported for ensemble measurements of simultaneously time- and wavelength-resolved fluorescence signatures with high resolutions in both parameters.[24−26] We report here the initial results from a time- and wavelength-resolved fluorescence microscope that permits the simultaneous measurement of the wavelength and emission time of every detected photon with *single molecule sensitivity*. The detection system relies on a commercially available multianode photomultiplier detector that is coupled to a custom readout scheme that allows the simultaneous measurement of the arrival position and arrival time of every detected photon at rates of several million photons per second. The arrival position is converted to wavelength, and both the absolute arrival time and the arrival time relative to the excitation laser pulse are recorded. Our approach is inherently a TCSPC technique with the added capabilities to time stamp and record the wavelength of each photon. Because these multiple parameters are simultaneously recorded for every detected photon, this technique is uniquely different from approaches that use, for example, an APD and a CCD camera to record the lifetime and spectrum, respectively. The APD/CCD camera combination measures spectral and temporal information on different photons rather than recording the wavelength and emission time for each photon. Hence the correlated information between lifetime and spectrum is lost. An example of this type of correlation, where the fluorescence lifetime depends on wavelength, is in a spFRET system as discussed below. In addition, a detection system such as a CCD camera that integrates photons for a time window loses the information on fluctuations that is contained in the time-stamped data stream from single photons.

We anticipate that the capabilities of time- and wavelength-resolved fluorescence microscopy to record correlations between the fluorescence emission time and spectrum will be particularly advantageous to understanding the dynamics of photophysical processes such as quenching, spectral diffusion, and energy transfer, which affect spFRET measurements and will potentially make spFRET measurements more quantitative. In addition, since this method records the arrival time (absolute and relative to laser excitation) and wavelength of each detected photon, the powerful statistical methods developed to analyze fluorescence fluctuations can now be extended to study spectral and lifetime fluctuations and their correlations.

In this paper, we present initial results on time- and wavelength-resolved fluorescence measurements of single rhodamine 6G (R6G), tetramethylrhodamine (TMR), and Cy3 molecules embedded in thin films of poly(methyl methacrylate) (PMMA). In the simplest demonstration, we use the technique to distinguish different fluorophores that have minimal differentiating fluorescence signatures in a sample environment. We also show results that demonstrate the powerful capability of simultaneously monitoring changes in the fluorescence spectrum, lifetime, and intensity of a single molecule as a function of time, providing new approaches to performing correlated fluorescence spectroscopy of single molecules. Finally, we present preliminary results of ongoing spFRET experiments in our laboratory using labeled polyproline peptides.

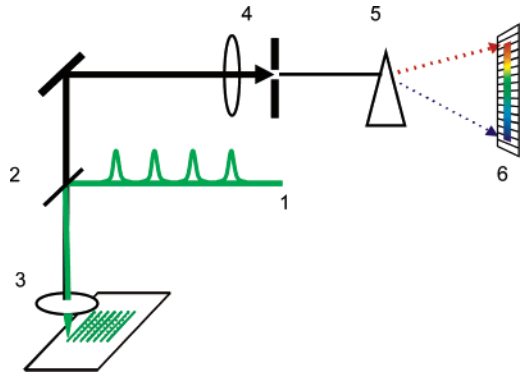

Figure 1. Schematic diagram of experimental setup: (1) excitation laser, (2) dichroic filter, (3) objective, (4) imaging optics and pinhole, (5) dispersing prism, and (6) time- and position-sensitive detector.

Experimental Section

Schematically shown in Figure 1, the experiment couples a conventional confocal fluorescence microscope setup to a custom photon detection system. The excitation beam comes from a 50 MHz repetition rate, picosecond mode-locked laser (Time-Bandwidth Products) producing 532 nm laser light. It is expanded to fill the back aperture of a plan-apochromat 60× oil immersion objective (NA 1.40, Nikon) to produce an approximately diffraction limited spot size on the sample. The average intensity of the laser excitation at the sample used for the experiments shown here is on the order of 1 kW/cm^2. The fluorescence emission is collected through the same objective. The excitation beam is passed through a broad-band $\lambda/4$ wave plate to make it circularly polarized at the sample so that molecular orientation effects are minimized. Fluorescence passes through a 532 nm dichroic filter (Chroma Technology Corporation) and a 532 nm Raman edge filter (CVI Laser), and is confocally imaged through a 75 μm pinhole. Fluorescence coming through the pinhole is collimated, dispersed by an AR-coated SF14 prism (<3% loss for both s/p polarizations, Optics For Research), and focused with a 75 cm cylindrical lens onto a position- and time-sensitive detector system. Sample scanning is accomplished with a piezoelectric-driven *xy* translation stage mounted on the inverted microscope (Nikon).

The time- and position-sensitive detection system is based on a commercially available multianode photomultiplier detector with 32 discrete elements (Hamamatsu Photonics, K.K.) coupled to custom readout electronics. The signals from the readout electronics are routed to constant fraction discriminators (CFDs) and finally to time-to-digital converters (TDCs). The timing electronics operate with the TDCs in the inverted mode, so the start is provided by the detection of a photon and the stop is provided by the next laser shot. Digital information from the TDCs on each photon is additionally time stamped to indicate the absolute arrival time with a resolution of 50 ns prior to transfer to a host computer. The readout scheme simultaneously records the arrival anode position, hence the fluorescence wavelength, and the emission time relative to the excitation pulse for each detected photon. The overall data acquisition system can run at megahertz photon rates, well above the count rates typically encountered in single molecule fluorescence microscopy. The wavelength range and spectral resolution are determined by the dispersion and the imaging geometry. For the experiments reported here a full spectral range of 140 nm in the visible region is used. Due to the nonlinear dispersion of the prism, the spectral resolution is approximately 3 nm at 540 nm and 5 nm at 650 nm. The overall instrument time response function has a full width at half-maximum (fwhm) of about 250

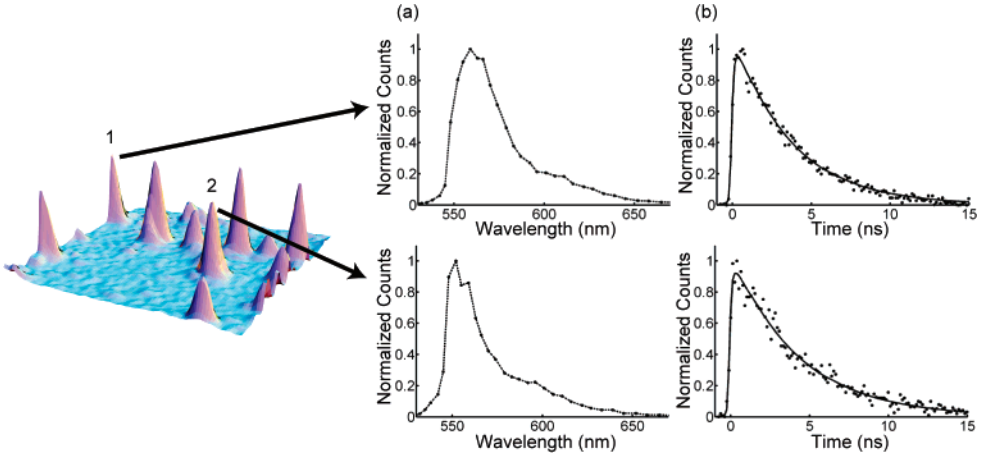

Figure 2. A 5 × 5 μm region of a mixed sample of R6G and TMR embedded in a thin layer of PMMA. Column a shows the fluorescence spectra, and column b shows the fluorescence lifetimes of the selected peaks. Solid lines in the lifetime plots are the monoexponential fits to the experimental data (circles). Peak 1 lifetime $\tau_1 = 3.58$ ns, and peak wavelength = 559 nm. Peak 2 lifetime $\tau_2 = 4.14$ ns, and peak wavelength = 552 nm.

ps; the TDC electronics record photon emission times with a precision of 16 ps. The time stamp system for recording the absolute time of arrival for each detected photon has a resolution of 50 ns. The detector assembly is cooled to approximately 0 °C, achieving a noise count of less than 10 Hz per anode element for a total dark count rate of <300 Hz.

The single dye molecule samples were prepared by mixing the dyes in a solution of 4 mg/mL PMMA in toluene to give a dye concentration of 0.1 nM. A small aliquot (50 μL) of this solution was deposited onto a clean glass coverslip and spin-coated to form a thin layer of PMMA. The coverslips were cleaned by immersing them in a 12% HF/ethanol solution for 5 s, rinsing with Nanopure water in two steps, and drying under nitrogen. The single molecule samples were made with Cy3 only, R6G only, TMR only, and a mixture of R6G and TMR. Samples for bulk measurements of the dye fluorescence were prepared the same way but using a 1 μM dye concentration in the PMMA/toluene solution.

The polyproline peptide samples were prepared in the laboratory of Dr. Haw Yang at the University of California, Berkeley. The peptide was synthesized with a carboxyl-terminal cysteine residue which reacts with the maleiimide derivative of the acceptor dye (Alexa 647, Invitrogen). The donor dye was attached to the N-terminus using the succinimidyl ester derivative of the donor dye (Alexa 555, Invitrogen). The labeling and the purification of the doubly labeled peptide were done according to the standard protocols. At the C-terminus, the synthesized peptide also contains a biotin molecule, which provides a strong attachment to a streptavidin-functionalized substrate. The streptavidine-functionalized substrate was prepared as follows. Plasma-etched coverslips were silanized and then activated with a poly(ethylene glycol) (PEG) mixture of 1:100 of PEG−biotin and PEG−succinimidyl propionate (PEG−SPA) in 0.1 M $NaHCO_3$ for 3 h. The coverslips were incubated for 10 min with a 0.2 mg/mL streptavidin (Invitrogen) solution in phosphate-buffered saline (PBS), and then incubated with 50 pM labeled polyproline in PBS for 10 min. Several washes with Nanopure water were performed between the different steps.

Images of samples were recorded by raster scanning the sample with the piezoelectric stage. For the image data shown, a series of scans were taken of 5 × 5 μm regions using 20 ms dwell time and 50 nm steps. Fluorescence time traces of individual molecules were also recorded. For the time traces, molecules were first located with a rapid raster scan of a 5 × 5 μm using 10 ms dwell time and 100 nm steps to avoid photobleaching the molecules. With the laser beam shuttered, the piezoelectric-driven stage was repositioned at the centroid of each cluster of bright pixels in the image corresponding to the location of a single molecule. The shutter was then opened and data were acquired for 25 s. The laser was immediately shuttered at the end of each 25 s collection time. The data acquisition was repeated until irreversible photobleaching occurred.

Results and Discussion

The distinguishing capability of this time- and wavelength-resolved fluorescence microscope is the ability to *simultaneously* measure the fluorescence emission wavelength and time for every detected photon with single molecule sensitivity. By synchronizing the raster scan of the piezoelectric-driven sample stage with the data acquisition, an image of the sample can be collected such that the fluorescence spectral information and temporal information are simultaneously recorded for every detected photon in each pixel. Figure 2 shows a three-dimensional fluorescence intensity plot of a 5 × 5 μm scanned region of a sample of mixed R6G and TMR dyes embedded in PMMA. The scan was taken with 50 nm pixels and 20 ms dwell time. This long dwell time and small pixel size was chosen to maximize the number of photons collected for each single molecule in a single scan. The region was scanned three consecutive times before a majority of the spots photobleached. Due to the very dilute (0.1 nM) concentration of the dye solution used to make the samples, most of the observed intensity peaks should represent single molecules. However, we also checked that the spatial fwhm's of the peaks are equivalent to a diffraction limited spot, and we confirmed that the peak intensities photobleached in a single step to the background level. The fluorescence emission spectrum and its associated decay trace for each pixel or group of pixels (appearing as a peak in the scanned image) can be generated by making histograms of the spectral and temporal data from every photon recorded in the selected pixel(s). A fluorescence decay for each of the 32 wavelength elements can actually be extracted from the data, but here only the overall decay is shown.

To the right of the intensity map in Figure 2 are the corresponding fluorescence spectra and decay plots for two selected single molecules as indicated by the arrows. These plots are generated from histograms of 25−30 thousand photon counts. These results demonstrate that the detection system is

TABLE 1: Fluorescence Characteristics of Bulk and Single R6G and TMR

	peak λ (nm)	τ (ns)
bulk R6G	552	3.80[a]
single R6G	552 ± 2.4[b]	3.75 ± 0.30[b]
bulk TMR	570	3.35[a]
single TMR	567 ± 8.3[b]	3.60 ± 0.40[b]

[a] Lifetime value is monoexponential fit of a single measurement. [b] Average of ~20 single molecules with ±standard deviation values.

capable of simultaneously measuring the fluorescence emission spectra and lifetimes from single molecules with an excellent signal-to-noise ratio. One use of these fluorescence signatures is to identify the corresponding fluorophores as discussed below.

To differentiate between R6G and TMR molecules in the above image scan, the distribution of fluorescence characteristics for single molecules of R6G and TMR embedded in PMMA were separately determined first. These results, from approximately 20 single molecules of each dye, along with the measurements of bulk dye samples in PMMA, are tabulated in Table 1. The bulk spectrum and decay values are in good agreement with those found in the literature for bulk R6G and TMR in PMMA.[27−29] Both the spectral peaks and the lifetimes of the two dyes are different enough from each other to distinguish between R6G and TMR in bulk samples in PMMA. However, while the average values of the fluorescence characteristics from single molecules correspond well with the bulk values, there is a small difference in the average fluorescence lifetimes of TMR. Assuming the bulk measurement is representative of the population mean, a statistical comparison to the mean of the single molecule TMR fluorescence lifetimes shows a significant discrepancy between the two values. This discrepancy between the bulk and single molecule TMR measurements likely arises from the effect of inhomogeneities in the polymer environment on the fluorescence characteristics of individual TMR molecules. Hence, the fluorescence lifetime is not a reliable parameter for discriminating between single R6G and TMR in the mixed single molecule sample.

The average fluorescence decay lifetimes are indistinguishable between the two types of single fluorophores in our sample. However, the simultaneously measured emission spectra of the two different dyes do provide means for discriminating between them. One simple approach is to consider the spectral peaks. The spectral peaks of single R6G molecules have a narrow distribution centered at 552 nm, while the spectral peaks for TMR molecules have a much broader distribution centered at 567 nm. On the basis of these characteristics, spot 1 in Figure 2 with emission peak at 559 nm can be assigned with high confidence to be a single TMR molecule because its spectral peak is statistically well outside the range observed for single molecule R6G molecules. The emission spectrum for spot 2 peaks at 552 nm, which is the same value as the average peak wavelength for single molecule R6G in PMMA. However, due to the wide spectral variation of TMR in PMMA, there is a small probability that this is a TMR molecule. With the simplifying assumption that the two distributions of spectral peaks are normal, we can assign a ~95% probability that the molecule at spot 2 is an R6G molecule. Clearly, more sophisticated methods for identification of fluorophores can be developed using the time- and wavelength-resolved data, including methods based on photon-by-photon analysis. These initial results emphasize the importance of characterizing the behavior of the individual fluorophores in the actual sample environment before analyzing mixed samples. This is especially

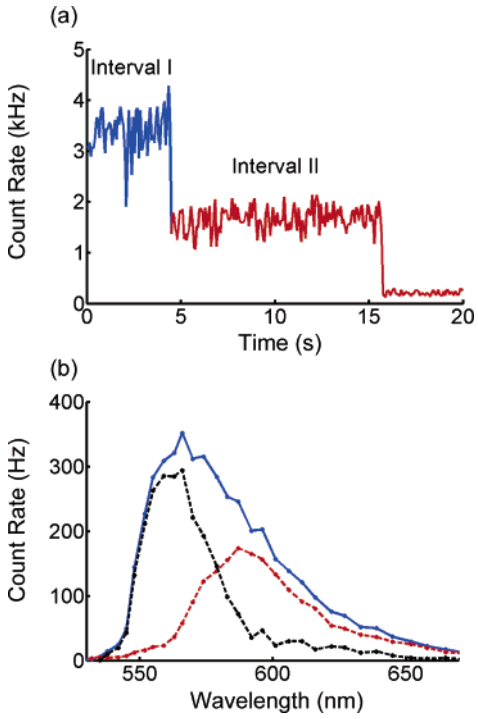

Figure 3. (a) Time trace, displayed in 75 ms time bins, for a diffraction-limited spot of a sample of TMR embedded in PMMA film. (b) Time-scaled fluorescence spectra for the time intervals I and II are shown by blue and red curves, respectively. The black curve is the difference spectrum between the two time-scaled fluorescence spectra.

critical since it is common to observe large spectral variations in single molecule measurements.[22,30−32]

This time- and wavelength-resolved fluorescence technique is also able to simultaneously measure the fluorescence spectral and temporal information for each detected photon as a function of acquisition time for individual molecules. The data described below are examples of time- and wavelength-resolved time traces from single image spots in samples of TMR and Cy3 in PMMA, and were chosen to illustrate the potential of the multiparameter technique to probe fundamental photophysics through correlated wavelength and lifetime measurements.

Of 50 measurements taken on TMR, only 20 were found to have simple time traces with single step drops in intensity to the background level. The remainder of the time traces exhibit fluctuations not easily described by a single step photobleaching process. Figure 3a shows an example of such a time trace from a single diffraction limited spot of TMR in PMMA sample. The observation of two discrete intensity steps in a time trace ending at the background level, as seen in the figure, is likely to be the sequential photobleaching of two molecules. However, the spectrally and temporally resolved data reveal a more complicated situation. If two molecules were present in the excitation volume, the data from time interval I should yield a fluorescence signature with contributions from both molecules. These contributions are independent if the molecules are not interacting. With one fluorophore photobleached, the emission spectrum from time interval II should only contain the signature of the single remaining fluorophore.

Because the emission wavelength and time relative to the excitation pulse are recorded for each photon, we can select different time intervals of the time trace and create a histogram of the fluorescence wavelengths and emission times of the photons arriving in that selected time region. This procedure results in a correlated fluorescence spectrum and lifetime map for that time interval. The fluorescence lifetime is almost the

same in the two intervals with values of 3.90 and 3.70 ns for intervals I and II, respectively. The fluorescence spectra, scaled by the acquisition time of the corresponding interval, for the two selected intervals of the time trace are shown in Figure 3b. These scaled spectra allow the examination of whether there are two molecules emitting in interval I. The scaled spectrum from interval II, where only one molecule is presumably emitting, is subtracted from the scaled total spectrum from interval I, where there may be two molecules emitting. The difference emission spectrum is typical of TMR in PMMA. This analysis is consistent with the notion that there were two noninteracting fluorophores with significantly different emission spectra in the focal volume. The fact that the scaled spectra from interval II can be subtracted from that in interval I to yield a spectrum that is positive everywhere and characteristic of TMR in PMMA is evidence that two molecules were initially present and that a TMR molecule photobleached at the end of interval I. However, the spectrum obtained in interval II is quite uncharacteristic of TMR in PMMA. This uncharacteristic spectrum, coupled with the observation that many trajectories of TMR molecules in PMMA did not show simple single step photobleaching, opens the possibility that the intensity change at the end of interval I is due to a photochemical change in a single TMR molecule that also causes a large shift in its emission spectrum. Thus, the time trace of Figure 3 does not definitively show the presence of two molecules in the detection volume. A more unambiguous conclusion regarding the presence of two fluorophores in the focal volume, however, can be reached using techniques such as photon antibunching, which we are currently implementing with this detection system.[33]

The data in Figure 4a show an example of a complex trajectory in which complete blinking implies the presence of only one molecule. This time trace was taken from a diffraction limited spot in a dilute (0.1 nM) sample of Cy3 embedded in PMMA in the same manner as were the R6G and TMR dyes. In this time trace plot, the count rate is high, ~5.50 kHz, during interval I, whereas the average count rate in interval II is ~1.50 kHz, a factor of 3.7 lower. Interval I ends with a single step drop to the background count rate, followed by a dark period of almost 1 s. Interval II starts with a single step rise after this dark period and ends 11 s later when the count rate again drops with a single step to the background level. The high count rate in interval I suggests there could be more than one molecule in the focal volume. However, the single step drop to the background level and the dark period are strong indications that only one molecule was present, because it is highly improbable that all the molecules blinked into the off state simultaneously and remained synchronously off for almost 1 s. Thus, it is concluded that the time trace of Figure 4a is taken from a single Cy3 molecule embedded in PMMA. Selecting the two different time intervals as indicated in the time trace plot, the fluorescence emission spectra and decay curves are generated and shown in parts b and c, respectively, of Figure 4.

Correlated with the large fluorescence intensity change, the fluorescence emission spectra and lifetimes of the single Cy3 embedded in PMMA also shifted significantly during the course of the time trace. The peak of the emission spectra shifted from 552 to 574 nm, with significant changes in the spectral shape. Simultaneously, the fluorescence lifetime dropped significantly from 3.30 to 1.70 ns. Thus, the red shift in the broad emission spectrum is correlated with a shift to shorter lifetimes. A possible explanation for a part of this observed correlation is that there was a change in the interaction of the Cy3 with its host site that resulted in faster nonradiative relaxation of the dye molecule. The change in the Cy3-host site interaction also caused the simultaneous red shifting of the emission spectrum and reduction of the overall fluorescence lifetime and quantum yield.

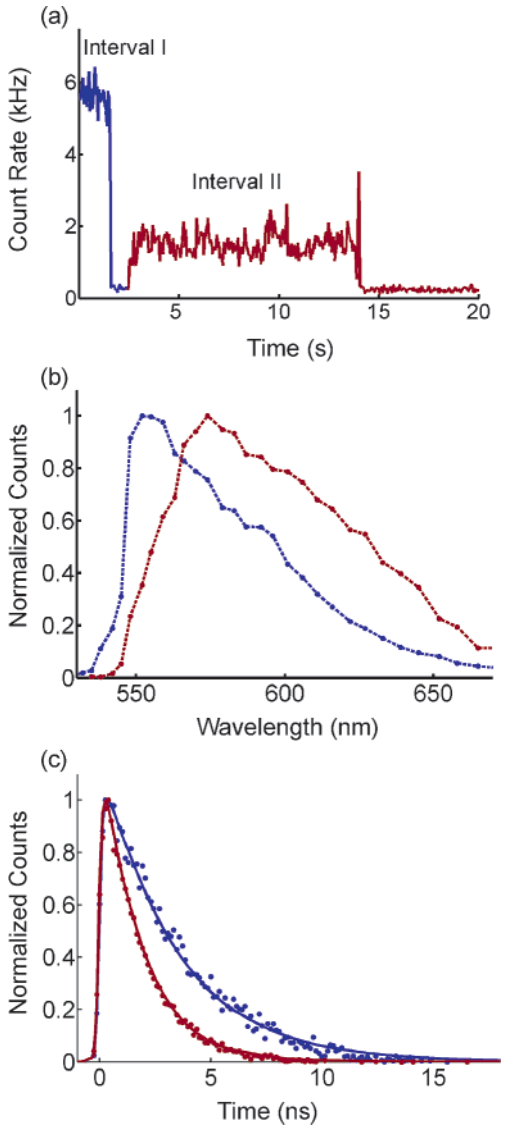

Figure 4. (a) Time trace, displayed in 75 ms time bins, for a diffraction-limited spot in a sample of dilute Cy3 embedded in a thin layer of PMMA film. (b) Normalized fluorescence spectra of the time intervals I and II are shown by blue and red curves, respectively. (c) The corresponding lifetime decays for the two time intervals are shown to fit to monoexponential curves: the blue curve for time interval I and the red curve for time interval II.

The observations above for an example single Cy3 molecule in PMMA are in sharp contrast to the static fluorescence characteristics observed for single Cy3 in PMMA, as shown by a few examples in Figure 5a,b. The single Cy3 molecules in PMMA exhibited wide spectral and temporal variations from molecule to molecule. However, there is a general trend that spectral peaks toward the red are correlated with longer fluorescence lifetimes, opposite that observed in Figure 4. This trend may be explained in part by the ν^3 dependence of the radiative lifetime on the fluorescence frequency. The correlation of spectrum and lifetime for individual single molecules may also be due to differences in the energy level of the fluorescing electronic state in different host sites. A lower energy of the fluorescing state of the dye molecule will result in a more red-shifted spectrum and also fewer nonradiative relaxation pathways, hence a lifetime that is longer.

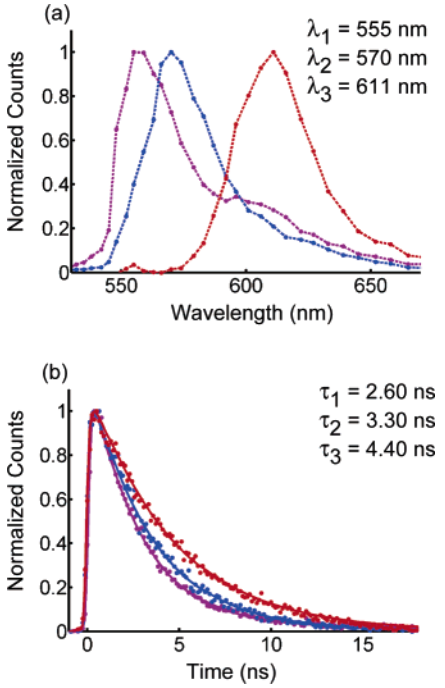

Figure 5. Fluorescence (a) spectra and (b) lifetime decays for individual single Cy3 molecules embedded in a thin layer of PMMA film.

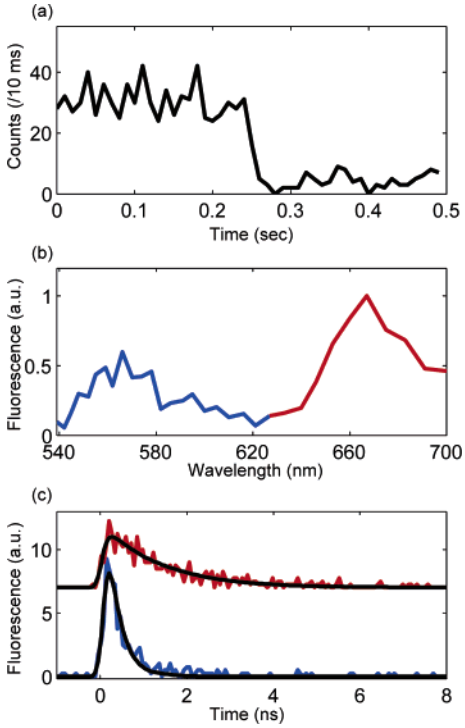

Figure 6. Single molecule FRET measurement on polyproline peptide labeled at the amino terminus with Alexa 555 (donor) and at the carboxyl terminus with Alexa 547 (acceptor). (a) The total intensity trajectory using donor excitation at 532 nm. (b) The emission spectrum corresponding to the first 250 ms of the trajectory. The donor contribution is shown in blue, and the acceptor is in red. (c) The fluorescence decays and their monoexponential fits (black curves) for the two spectral features: in blue, $\tau_{don} = 0.27 \pm 0.03$ ns, and in red, $\tau_{acc} = 1.29 \pm 0.18$ ns.

As alluded to in the Introduction, the time- and wavelength-resolved fluorescence microscope is ideally suited to studying the dynamics of photophysical processes such as those in single-pair FRET. In this example, we used short polyproline peptides as molecular spacers between donor Alexa 555 and acceptor Alexa 647 fluorophores. Polyproline is assumed to be a rigid rod, and was used as a spacer by Stryer and Haugland to check experimentally the dependence of the FRET rate on the donor−acceptor distance.[34]

Figure 6a shows the fluorescence intensity time trace of an spFRET on a polyproline peptide containing 24 proline residues. The sudden decrease of the signal after ~250 ms to background level (step photobleaching) is indicative of a single molecule intensity trajectory. The correlated fluorescence emission and decay spectra for the spFRET are shown in parts b and c, respectively, of Figure 6. The fluorescence emission spectrum has two clearly separated peaks around 565 and 670 nm. Without the use of any band-pass filters, fluorescence properties can be analyzed after acquisition according to the actual emission characteristics of the donor and the acceptor. In this case, we chose 627 nm as the delimiting emission wavelength between the donor, to the blue, and the acceptor, to the red. Since the emission time of every photon is also recorded simultaneously with the emission wavelength, the decay traces directly correlated to the two different emission spectra features can easily be determined. The decay traces for the donor and for the acceptor are represented by blue and red curves in Figure 6c, respectively. The fluorescence lifetimes obtained by monoexponential fitting of the decay curves are markedly different, namely 270 ps for the donor and 1.29 ns for the acceptor. The 60% FRET efficiency for this spFRET system, which was computed based on the above spectrum split, is in good agreement with the theoretical value computed based on molecular parameters of the polyproline and the Förster radius of the donor−acceptor pair. To our knowledge, this is the first measurement of the correlated spectrum and decay associated with an spFRET process. Using our setup, the *intrinsic correlation* between the temporal and spectral quantities is directly measured. From the correlated data one can construct, post acquisition, *any* combination of time-gated spectra or wavelength-gated decays and extend the powerful techniques of correlated photon statistics to gain additional insights into the system.

The examples presented here are to demonstrate the distinctive strength of a simultaneous time- and wavelength-resolved fluorescence microscope to record spectral and temporal fluctuations of fluorophore characteristics in a correlated manner, one photon at a time. While it is not the intention of this paper, it is clear that a thorough examination of the photophysics behind these examples requires an analysis of many single molecule time traces and various controlled host environments.

Conclusion

This paper describes initial results from a simultaneous time- and wavelength-resolved single molecule confocal microscope system. Correlations between the fluorescence intensity, wavelength, and emission time are observed in these experiments through the simultaneous measurement of the fluorescence wavelength and emission time for individual detected photons. It is shown that these measurements can be made at the single molecule level, providing correlated fluorescence properties that characterize single molecule systems at a new level of detail. This detection technique has the capability to record correlated fluctuations in single molecule fluorescence spectra and lifetimes on time scales that are limited only by the photon emission rate obtainable from the sample. Thus it is well-suited for studying dynamics of processes that change the local environment of fluorophores and hence their fluorescence characteristics. Perhaps the most obvious application of this method is in studies

of spFRET where the fluorescence spectra and fluorophore lifetimes are inherently correlated by the dynamics of the energy transfer process. We have shown here preliminary results from spFRET experiments. Detailed experiments on spFRET in conjunction with development of data analysis techniques that take advantage of the multicorrelated information are currently underway in our laboratory.

Acknowledgment. The authors thank Prof. Haw Yang of the University of California, Berkeley, for graciously providing the labeled polyproline samples, and M. Gutzler for expert technical assistance. This research is supported by Sandia National Laboratories LDRD and the Division of Chemical Sciences, Geosciences and Biosciences, the Office of Basic Energy Sciences, U.S. Department of Energy. Sandia is a multiprogram laboratory operated by Sandia Corporation, a Lockheed Martin Company, for the United States Department of Energy's National Nuclear Security Administration under Contract No. DE-AC04-94AL85000.

References and Notes

(1) Michalet, X.; Kapanidis, A. N.; Laurence, T.; Pinaud, F.; Doose, S.; Pflughoefft, M.; Weiss, S. *Annu. Rev. Biophys. Biomol. Struct.* **2003**, *32*, 161.

(2) Moerner, W. E. *J. Phys. Chem. B* **2002**, *106*, 910.

(3) Nie, S.; Zare, R. N. *Annu. Rev. Biophys. Biomol. Struct.* **1997**, *26*, 567.

(4) Xie, X. S.; Trautman, J. K. *Annu. Rev. Phys. Chem.* **1998**, *49*, 441.

(5) Becker, W.; Hickl, H.; Zander, C.; Drexhage, K. H.; Sauer, M.; Siebert, S.; Wolfrum, J. *Rev. Sci. Instrum.* **1999**, *70*, 1835.

(6) Li, L.-Q.; Davis, L. M. *Rev. Sci. Instrum.* **1993**, *64*, 1524.

(7) Minami, T.; Kawahigashi, M.; Sakai, Y.; Shimamoto, K.; Hirayama, S. *J. Lumin.* **1986**, *35*, 247.

(8) Wilkerson, C. W.; Goodwin, P. M.; Ambrose, W. P.; Martin, J. C.; Keller, R. A. *Appl. Phys. Lett.* **1993**, *62*, 2030.

(9) Watkins, L. P.; Yang, H. *Biophys. J.* **2004**, *86*, 4015.

(10) Xie, X. S. *J. Chem. Phys.* **2002**, *117*, 11204.

(11) Yang, H.; Xie, X. S. *J. Chem. Phys.* **2002**, *117*, 10965.

(12) Prummer, M.; Hübner, C. G.; Sick, B.; Hecht, B.; Renn, A.; Wild, U. P. *Anal. Chem.* **2000**, *72*, 443.

(13) Ha, T.; Enderle, T.; Ogletree, D. F.; Chemla, D. S.; Selvin, P. R.; Weiss, S. *Proc. Natl. Acad. Sci. U.S.A.* **1996**, *93*, 6264.

(14) Tinnefeld, P.; Herten, D.-P.; Sauer, M. *J. Phys. Chem A* **2001**, *105*, 7989.

(15) Deniz, A. A.; Dahan, M.; Grunwell, J. R.; Ha, T.; Faulhaber, A. E.; Chemla, D. S.; Weiss, S.; Schultz, P. G. *Proc. Natl. Acad. Sci. U.S.A.* **1999**, *96*, 3670.

(16) Ha, T.; Ting, A. Y.; Liang, J.; Deniz, A. A.; Chemla, D. S.; Schultz, P. G.; Weiss, S. *Chem. Phys.* **1999**, *247*, 107.

(17) Hohng, S.; Joo, C.; Ha, T. *Biophys. J.* **2004**, *87*, 1328.

(18) Sabanayagam, C. R.; Eid, J. S.; Meller, A. *Appl. Phys. Lett* **2004**, *84*, 1216.

(19) Hernando, J.; van der Schaaf, M.; van Dijk, E. M. H. P.; Sauer, M.; Garcia-Parajo, M. F.; van Hulst, N. F. *J. Phys. Chem A* **2003**, *107*, 43.

(20) Schaffer, J.; Volkmer, A.; Eggeling, C.; Subramaniam, V.; Striker, G.; Seidel, C. A. M. *J. Phys. Chem. A* **1999**, *103*, 331.

(21) English, D. S.; Harbron, E. J.; Barbara, P. F. *J. Chem. Phys.* **2001**, *114*, 10479.

(22) Lu, H. P.; Xie, X. S. *Nature* **1997**, *385*, 143.

(23) Weston, K. D.; Burrato, S. K. *J. Phys. Chem. A* **1998**, *102*, 3635.

(24) Courtney, S. H.; Wilson, W. L. *Rev. Sci. Instrum.* **1991**, *62*, 2100.

(25) Kelly, L. A.; Trunk, J. G.; Sutherland, J. C. *Rev. Sci. Instrum.* **1997**, *68*, 2279.

(26) Tramier, M.; Gautier, I.; Piolot, T.; Ravalet, S.; Kemnitz, K.; Coppey, J.; Durieux, C.; Mignotte, V.; Coppey-Moisan, M. *Biophys. J.* **2002**, *83*, 3570.

(27) Deshpande, A. V.; Namdas, E. B. *J. Lumin.* **2000**, *91*, 25.

(28) Lee, M.; Tang, J.; Hochstrasser, R. M. *Chem. Phys. Lett.* **2001**, *344*, 501.

(29) Lee, M.; Kim, J.; Tang, J.; Hochstrasser, R. M. *Chem. Phys. Lett.* **2002**, *359*, 412.

(30) Geva, E.; Reilly, P. D.; Skinner, J. L. *Acc. Chem. Res.* **1996**, *29*, 579.

(31) Novotny, L. *Appl. Phys. Lett* **1996**, *69*, 3806.

(32) Wazawa, T.; Ishii, Y.; Funatsu, T.; Yanagida, T. *Biophys. J.* **2000**, *78*, 1561.

(33) Basché, T.; Moerner, W. E.; Orrit, M.; Talon, H. *Phys. Rev. Lett.* **1992**, *69*, 1516.

(34) Stryer, L.; Haugland, R. P. *Proc. Natl. Acad. Sci. U.S.A.* **1967**, *58*, 719.